High-Frequency Current Interruption of Vacuum Interrupters in an Experimental DC Circuit Breaker

N. A. Belda[1,2]*, R. P. P. Smeets[1], R. M. Nijman[1], M. Poikilidis[3] and C. A. Plet[3]

[1] KEMA Laboratories, DNV GL, the Netherlands, [2] Technische Universität Darmstadt, Germany
[3] Transmission and Distribution Technology, DNV GL, the Netherlands
* nadew.belda@dnvgl.com

***Abstract*—Recently, several manufacturers have proposed and developed prototypes of high-voltage direct current (HVDC) circuit breakers (CBs) based on various dc current interruption principles. However, due to a lack of operational experience with this type of equipment, no clearly defined requirements that these new developments should satisfy exist. To define and refine justified test requirements, a thorough understanding of the interactions between the internal components of the HVDC CBs and the stresses on these components is necessary. For this purpose, an experimental dc CB based on the active current injection technique is setup in a high-power laboratory. The contribution of this paper focuses on the performance of vacuum interrupters (VIs) for dc CB application. The performances of three different VIs, designed for ac application, are investigated. About 200 tests, under different test conditions, have been conducted in which up to 850 current zero crossings (CZCs) are created. The test results are analyzed and presented in detail along with statistical information obtained from the analysis of the measured parameters. The test results serve to identify the critical stages of current interruption process that need to be demonstrated during typical current interruption tests of HVDC CBs. It is found that the three types of VIs behave very differently; the rate-of-change of current near CZCs is not the only key parameter; and successful current interruptions can still be achieved after re-ignitions and re-strikes.**

I. Introduction

High-voltage dc circuit breakers (HVDC CBs) are expected to play an important role in the protection of multi-terminal and meshed voltage source converter (VSC) HVDC grids [1]. Several concepts of HVDC CBs have been proposed and some are prototype tested [2]–[10]. A few cases have been put in service in radial multi-terminal VSC-HVDC pilot projects in China. For example, 200 kV hybrid HVDC CBs have been installed and commissioned at Zhoushan five terminal radial HVDC grid [8], [9], whereas 160 kV active current injection HVDC CBs have been put in operation in Nan'ao three terminal radial HVDC grid [10], [11].

The use of HVDC CBs at the ends the transmission lines enable selective clearing of dc line faults whilst ensuring uninterrupted power flow in the healthy part of the grid. The requirements the HVDC CBs are, ultimately, determined by the functional specification of the HVDC grid in which they are installed. Given the progresses in the developments of the power electronic components of a converter, the HVDC CBs are expected to clear a dc line fault rapidly to minimize the blocking of the converters even close to a fault location [12]. The fact that the converters are not blocking during fault current clearing process incurs additional burdens to the HVDC CBs in terms of peak interruption current, the duration of the transient interruption voltage (TIV) and the energy that it has to absorb [12]–[14].

So far the testing of HVDC CBs focus on the proof of a concept such as verifying internal current commutation and the TIV generation. However, in service, the HVDC CBs are subjected to much more stresses than just these. The important stages of fault current interruption process that the HVDC CBs need to demonstrate during a current interruption process are described in [3]. Four critical current interruption stages are identified−internal current commutation, TIV generation, system energy absorption and DC voltage withstand after current suppression. So far the challenge of testing the HVDC CBs has been twofold. Firstly, no international standards specifying test requirements exist. Secondly, no test circuit capable of supplying adequate and complete stress on the HVDC CBs are used at this stage of development [15].

In order to refine and define justified test requirements, thorough understanding of the interactions of the internal components of HVDC CB and the stresses on these components under real power condition is necessary. For this purpose, an experimental dc CB based on active current injection technique is set-up in the high-power laboratory. The experimental dc CB uses commercial ac vacuum circuit breakers (VCBs) as the main interrupter. A test circuit based on ac short-circuit generators capable of supplying a range of stresses on dc CB is used. The details of the test circuit have been discussed in [3]. Using this test circuit, the performance limits of the main components, namely, the vacuum interrupter (VI) and the metal oxide surge arrester (MOSA), which are common to most technologies of HVDC CBs are investigated. The contribution of this paper focuses on the performance of VI(s) for dc current interruption. Three supposedly different designs of VIs are investigated. Large number of tests have been performed under various test conditions to identify the critical parameters having an impact not only on the performance of a VI(s) but also on the overall performance of a dc CB.

The remainder of the paper is organized as follows. In Section II, the test setup of the experimental dc CB along with its configuration and technical specification is presented. The test results are analyzed in detail for all the three types of VIs in Section III followed by discussion of the overall statistics in Section IV. Finally the conclusion

978-1-7281-5218-9/19/$31.00 ©2019 IEEE

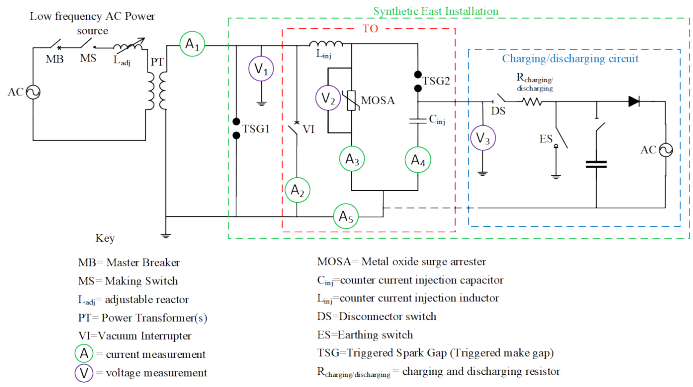

Fig. 1: Electrical layout of the experimental dc CB test setup

based on the results of the paper is presented in SectionV.

II. Test Setup and Design of the Experimental dc CB

A. Test setup

The experimental dc CB is setup with a focus on the investigation of stresses on the internal sub-components. Here, the overall speed of operation of the dc CB is not the main objective. This is due to the fact that the components of the experimental dc CB, specifically the mechanisms/drives of the VCBs used are not designed for dc CB application, rather for ac CB application which is slower[1]. The test parameters, however, are the same parameters used for the testing a real dc CB.

The electrical layout of the test setup is shown in Fig. 1. The main components of the experimental dc CB are shown in the dashed red box in the figure. It consists of a VI or series connected VIs in the main current path, a pre-charged capacitor (C_{inj}) which supplies a counter injection current for artificial current zero creation, an inductor in the injection path (L_{inj}) which is used to limit the frequency and the peak value of the injection current, the triggered spark gap 2 (TSG2) that serves as a high-speed making switch and finally the MOSA, which is a crucial component for limiting and maintaining the TIV across the dc CB during current suppression and hence, absorbing the energy in the circuit. The circuit on the right most side of Fig. 1 is the charging and discharging circuit for the injection capacitor. Fig. 2 depicts the photo of the laboratory setup of the experimental dc CB with the main components labeled.

B. Technical Specification of the Experimental dc CB

The performance of a VI at different stages of the current interruption process depends on the contact design, contact materials, contact composition, arc control, etc., [16]. In order to investigate the impacts of the differences in the design of the VI contacts, three different, standard off-the-shelf VCBs produced by various manufacturers are used. These are all three-phase ac CBs with ratings as shown in Table I.

[1]The practical dc circuit breaker is required to secure sufficient contact gap to clear a dc fault within a specified fault neutralization time.

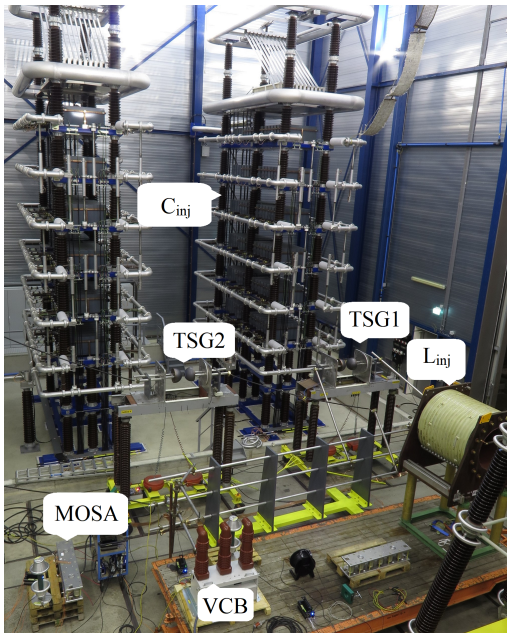

Fig. 2: Laboratory setup of the experimental dc CB

In order not to exceed the ac voltage ratings of the VCBs, which is in the range between $36-38\ kV_{RMS}$ (see Table I), the TIV (and hence the MOSA clamping voltage) of a single interrupter dc CB is chosen to be 40 kV with transient peak as high as 45 kV. For the single interrupter case, only one out of the three poles (VIs) is used while the remaining poles are not connected to the circuit. The electrical layout of a single interrupter dc CB is shown in Fig. 3a. In order to double the voltage rating (thus, the TIV) of the experimental dc CB, two VIs (the peripheral poles) are connected in series as shown in Fig. 3b. To ensure the doubling of the TIV, two series connected MOSA stacks are used. The current rating remains the same as for the single interrupter case. Nevertheless, the charging voltage as well as the value of the C_{inj}, and the size of L_{inj} are adjusted to keep the electrical stresses per component the same as for the single interrupter case. For the double interrupter setup there are voltage grading capacitors across each VI to ensure equal distribution of the TIV. The effectiveness of different values of grading capacitors is also investigated.

In the arrangement depicted in Fig. 3a & 3b, the MOSA is connected in parallel with the C_{inj}. Alternatively, it could be connected in parallel with the VI(s) as well; however, this results in a high-frequency damped oscillation superimposed on the TIV during current commutation into the MOSA. This is because by the time the C_{inj} is charged to the clamping voltage level of the MOSA, the system current still flows through the L_{inj}. Since the commutation of current from a reactor is not instant, the C_{inj} keeps charging until the current commutation from the L_{inj} is completed. The C_{inj} voltage appears across the VI. Therefore, to reduce the voltage stress on the VI due to the transient overshoot during current commutation from L_{inj}, the arrangement shown in Fig. 3 is chosen. In this case there is no need of current commutation from the L_{inj} to the MOSA during the entire current suppression

TABLE I: Specifications of VCBs used in the experimental dc CB

VCB Type	rated voltage (*kV*)	rated current (*A*)	rated short-circuit current (*kA*)	opening time (*ms*)
A	38	2500	31.5	37.5
B	36	2500	40	46.6
C	36	2000	31.5	37

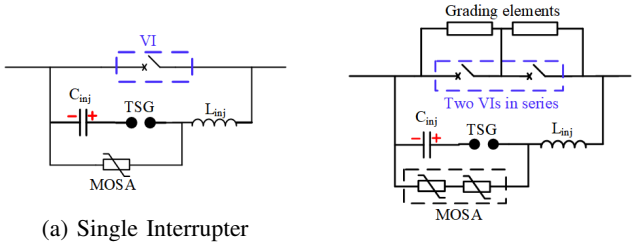

(a) Single Interrupter

(b) Double Interrupter

Fig. 3: Electrical diagram of experimental dc CB

period.

C. Test method and procedure

The stresses seen by the VI(s) depend on the magnitude of interruption current. Since it is not obvious that interruption at low current is less severe than high current, a range of interruption currents has been investigated as follows.

1) Low current −2 kA
2) Medium current−10 kA
3) High current−16 kA

In fact, there are several other parameters whose impacts are investigated at each of the tests. Tests are repeated 10 times by keeping the parameters of interest, for example, the arcing duration at each test.

A test current is supplied by ac short-circuit generators operated at low power frequency as discussed in [3]. An example of the prospective current produced during a test is shown in Fig. 4 along with different timing signals. The test object (the experimental dc CB) is operated in such a way that the contacts of the VI(s) are separated after the short-circuit current starts to flow. This means the VCB needs to be tripped at T_1[2], prior to the onset of the prospective current which is at T_2. The breaker opening time which is the duration from T_1 until T_3 is precisely known for the VCBs, see Table I. Therefore, the trip command can be precisely sequenced in reference to the moment of short-circuit application as illustrated in Fig. 4. At T_4 the counter current is injected from the C_{inj} at a frequency of 4 kHz with peak value of 20 kA ($\pm 5\%$). Due to inherent losses in the circuit the current from the injection circuit decays quickly while the system current keeps rising. This limits the number of CZCs that can be created during current interruption. Thus, the injection circuit parameters are selected so that at least 4 CZCs can be created during high-current test.

[2]During the testing of the proper dc CBs, a trip command is sent after a short circuit is applied to mimic the actual application

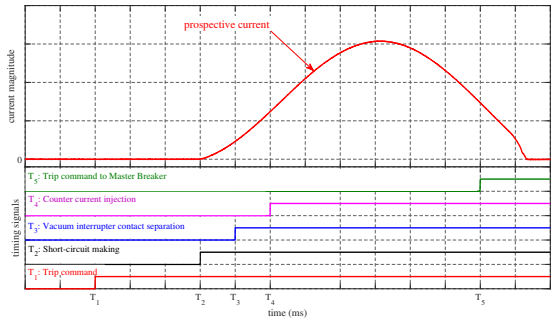

Fig. 4: Test method and procedure: prospective current and timing diagrams

III. Test Results Analysis

It must be noted that the discussions in the paper are entirely based on the observation during the experimental test campaign using the interrupters of commercial ac VCBs described above. The test results could be different for a real HVDC CBs which use special VIs optimized for the purpose of dc current interruption. Besides, the real HVDC CBs use very fast operating mechanisms which can achieve sufficient contact gap for successful current interruption within a specified current neutralization time [17].

A. Test Results of VCB Type A

Typical 10 kA current interruption by a single VI of VCB type A is shown in Fig. 5. Current and voltage measurements near CZCs are shown in the zoomed plots. The contacts of the VI separate at T_3 followed by current conduction via vacuum arc. The system current at T_3 is 7.1 kA and rising. One of the crucial parameters determining the probability of current interruption is the $arcing\ duration$ of the VI−the duration between the moment of contact separation until the 1^{st} CZC. It is related to the gap length between the contacts and hence, to the dielectric recovery of the VI(s), although the relationship to the latter is not linear [16]. For the test result shown in Fig. 5, the arcing duration until the 1^{st} CZC is 2.9 ms even though the current interruption occurred at the 8^{th} CZC after a total of 3.7 ms arcing. This means the VI re-ignited during the first 7 CZCs. There are increasing (although not monotonic) re-ignition voltage spikes with alternating polarities seen in the Fig. 5a. This shows that the VI is indeed attempting to interrupt the current at each CZC.

The re-ignition voltage spikes are due to the charge remaining on the C_{inj} at the moments of CZCs, referred to as initial TIV (ITIV). This is the main cause of re-ignitions at CZCs especially when interrupting low currents suggesting a dielectric, rather than a thermal breakdown phenomenon. In reality, except at the 8^{th} CZC, the re-ignitions occur before the entire ITIV appears across the VI. The increase in the re-ignition voltage at successive CZCs is due to the increased contact gap and, at the same time, the decreased rate-of-change of current (di/dt) near CZC. The latter is mainly caused by the damping in the counter injection current and, to some extent, by a slight

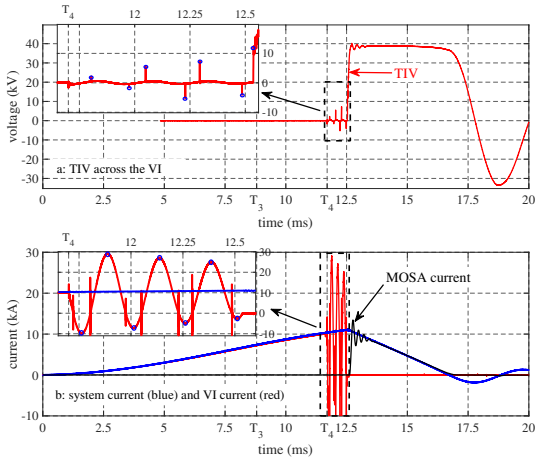

Fig. 5: Current interruption by experimental dc CB−VCB type A

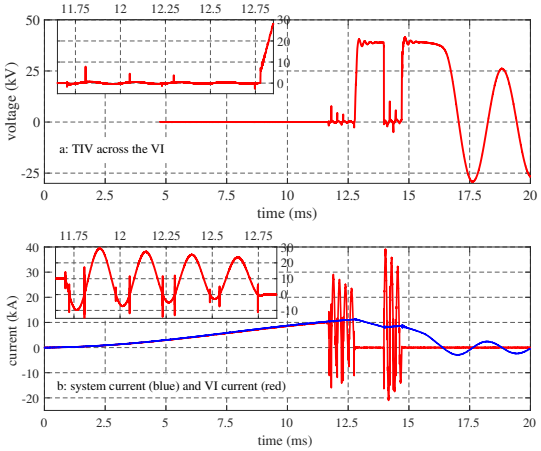

Fig. 6: Late restrike in the VI during fault current suppression period

increase in the system current. The lower di/dt means the VI has more time for cooling of the arc.

From the zoomed portion of Fig. 5b, it can be seen that, because of superposition of the system current and the injection current, the current through the VI oscillates between high positive and low negative values (shown by blue circles at local peaks). This results in major loop and minor loop currents between successive CZCs and this has significant impact on the probability of a re-ignition at a CZC. There are two main causes for a re-ignition at a CZC; thermal and dielectric, the former being dominant after the major loop current flow. For example, the re-ignition at the 1^{st} CZC is entirely caused by thermal effect as there is no observable re-ignition voltage. At the 2^{nd} CZC, however, a re-ignition voltage of about 2.2 kV is observed. The crucial parameters near CZCs including the major and minor loop current durations are shown in Table II.

TABLE II: Parameters near CZCs during current interruption by a VI for the example case shown in Fig. 5

CZC number	1	2	3	4	5	6	7	8
di/dt ($A/\mu s$)	498	44	371	365	295	286	209	206
peak current[3] (***kA***)	10.1	9.8	29.2	7.2	27.2	5.0	25.3	2.7
loop duration (μs)	2890[4]	83.7	170	75.2	180	64.1	191	51.3
ITIV (***kV***)	Negl.	2.2	-1.6	5.5	-5.26	7.3	-4	12.5

From the moment of local interruption at the 8^{th} CZC onwards, the short-circuit current is fully commutated to the injection branch of the dc CB, thus charging the C_{inj} until the clamping voltage of the MOSA is reached. Henceforth, the MOSA maintains a more or less constant TIV voltage, see Fig. 5a, until the system current is suppressed. Even if there is no thermal energy being injected into the VI contact gap at this stage, the VI must withstand the TIV during current suppression and subsequently the system voltage after current suppression is over.

Nevertheless, it was observed on numerous occasions that the VI fails to sustain the TIV for sufficient duration after local current interruption. Henceforth, this kind of failure is referred to as a re-strike. In most of the cases a re-strike occurs before the capacitor is charged to the clamping voltage of the MOSA. However, in some cases a (late)re-strike can occur even after sustaining the peak TIV. Again this phenomenon depends on the design, contact material, contact gap and pre-conditioning of the VIs. Fig. 6 shows a test result in which a (late)re-strike occurred during the current suppression period. As can be seen from the figure, the re-strike happened about 1.2 ms after local current interruption. During this time, the system current has been suppressed by about 3 kA from its peak value. After the re-strike the system current starts to rise again although the VI could clear before the system current exceeds the previous peak value. This is a unique feature of dc CBs based on current injection technique that a re-strike does not necessarily lead to a complete failure to interrupt since the vacuum gap interrupts and restores insulation. The main impact of a re-strike in this case is a longer total current interruption period and an increased energy absorption in the MOSA. However, this is not always the case and the VI may not be able to clear after a re-strike which was also observed on numerous occasions during the test campaign. It can be seen from Fig. 6 that the oscillating current after the occurrence of the re-strike has a higher amplitude than before the re-strike. This is because the C_{inj} is charged to the TIV which is normally 50% higher than the pre-charge voltage. Hence, the parameters near the CZCs including the di/dt, the duration and the local peak values of the loop currents are also increased by 50% compared to the corresponding values before the re-strike. Moreover, the local current interruptions (both before and after the re-strike) occurred after minor loop currents. In fact, for the VI type A, there are only a few cases where current interruption occurred on the 1^{st} CZC or after the major loop current. For example, among 98 tests (includes single and double interrupter tests), only 6 times the VI(s) could interrupt at the 1^{st} CZC. In the 92 tests in which the 2^{nd} CZC was created, about 25% of the cases the VI(s) could clear whereas of the total 3^{rd} CZCs created only in less than 3% the VI(s) could interrupt. It is found that VI(s) tends to clear current after minor loop current (even numbered CZCs), see Fig. 7, and even after the occurrence of a re-strike. In general, a closer scrutiny of all the test results show that the re-ignition voltage is higher after minor loop

[3]the peak value prior to a CZC

[4]arcing duration from contact separation until the 1^{st} CZC

current than after major loop current.

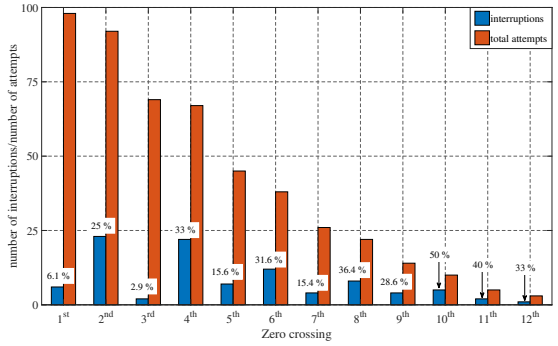

Fig. 7: Proportion of current interruption at a given CZC number

Another important observation is the impact of the di/dt on the current interruption performance of the VI(s). It can be seen from Fig. 8 that in no circumstance the VI of type A could clear when the di/dt is higher than 620 A/μs. Although the arc time constant of a VI is very short, it has a lower limit. When a CZC is created before the arc cools down, it leads to re-ignition[5]. It must be noted that the chance of a re-ignition is not determined only by the di/dt at a CZC and current peak prior to it but also by the other parameters such as the total arcing duration. For example, the re-ignitions observed at low di/dt are mainly caused by a short arcing duration when interrupting high current tests. Moreover, at times the arcing duration was intentionally decreased to 1.5 ms and the VI(s) never interrupted at CZCs which occurred before 2.9 ms arcing.

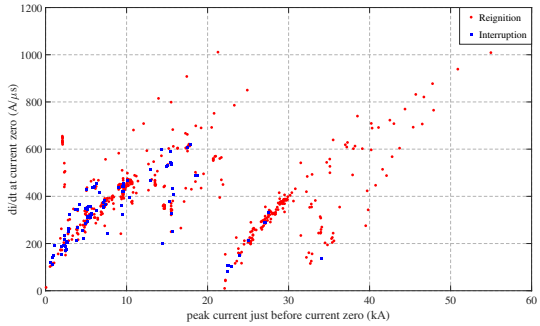

Fig. 8: Current interruption versus re-ignition as a function of the di/dt of current near CZCs and peak value of current prior to CZCs

B. Test Results of VCB Type B

Similar tests were performed using VCB type B while keeping the rest of the circuit components and the test parameters as for VCB type A. For VCB type B, there is a slight scattering in the moment of contact separation of its interrupters and hence, the precise control of the arcing duration is difficult. The performance of the VI of type B is, however, completely different than that of type A. For example, in about 75% of the tests the VI of type B interrupted the current at the 1^{st} CZC and, sometimes even at shorter arcing durations compared to the VI of type A. In about 16% of the tests, this VI failed to interrupt the current. More than half the failure occurred during the high-current tests by a single interrupter setup. In a single interrupter setup, the high-current test was performed 12 times of which 6 times the VI failed to clear even if the arcing duration until the 1^{st} CZC is prolonged to 3.48 ms. In this case 4 CZCs are created and the arcing duration until the last CZC is 3.78 ms. Unlike the VI of type A whose performance improve along the number CZCs, see Fig. 7, the major attempt to clear by VI of type B is at the 1^{st} CZC. This is observed in all the unsuccessful interruption test results where the highest re-ignition voltage is seen at the 1^{st} CZC. In fact, there are attempts to clear on the later CZCs but it re-ignited at lower voltage than at the 1^{st} CZC.

A general observation from the unsuccessful interruption test results (considering a single interrupter case) is that as the arcing duration increases, the re-ignition voltages at the CZCs also increase. This confirms the VI's attempt to clear improve with longer arcing duration. Successful current interruption was achieved when the arcing duration until the 1^{st} CZC is prolonged to 3.6 ms. All the tests with arcing durations longer than 3.6 ms resulted in successful interruption and, in all the cases, upon the 1^{st} CZC. The main conclusion from the test results is that, for a given rated interruption current, there is a minimum arcing duration that needs to be ensured before the CZ creation for the VI of type B. However, this might be improved to some extent by high-speed contact drives such as electromagnetic actuators [17].

However, for a double interrupter setup of type B, there was no overall interruption failure recorded while in a few cases re-ignitions and re-strikes occurred especially at low current interruption tests. Fig. 9 shows low current interruption by double interrupters setup of type B VIs.

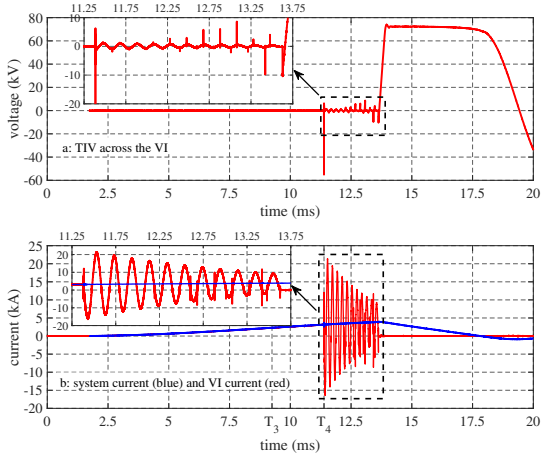

Fig. 9: Low current interruption by double interrupter of VI type B

It can be seen that the most severe attempt to clear the current is on the 1^{st} CZC at which re-ignition occurred at -55 kV ITIV. After the re-ignition there is not observable attempt to clear until after the 10^{th} CZC. From the 10^{th} CZC onwards, there is an increasing ITIV observed until the interruption occurred at the 23^{rd} CZC. The large ITIV observed at the 1^{st} CZC is due to the significant proportion

[5]The peak current values in excess of 20 kA observed in the figure are due to superimposed injection current on to the system current. These are the peak values of the major loop currents

of charge remaining on the C_{inj} when interrupting low current. This is the main cause of re-ignitions when interrupting low current tests. This becomes severe for the double interrupter case especially when equal voltage grading across the VIs is not ensured. Actually there are numerous occasions in which a re-ignition/re-strike occurs in one of the VIs but did not lead to overall re-ignition/re-strike because the second VI could handle the entire stress.

C. Test Results of VCB Type C

Similar to VCB type B, VCB type C also has a slight dispersion in the opening time. In some cases this has resulted in unintentional sub-millisecond arcing durations. For a single interrupter test setup, only 10 kA current interruption tests have been performed at different arcing durations. For all the tests in which the arcing duration is in the range between 3.76−4.48 ms, the VI cleared on the 1^{st} CZC and no re-strike was observed. However, when the arcing duration is in the range between 0.3−1.6 ms, re-strikes were observed on a few occasions which finally led to failed interruptions. Fig. 10 shows a test result in which a re-strike occurred in the VI of type C. A critical observation in this case is that a re-strike occurred not during the test with the shortest arcing duration, rather during a test with the longest arcing duration from the set, i.e. 1.6 ms, although a re-strike is also observed in another test with arcing duration of 0.44 ms. In both cases the VI failed to clear after the re-strikes even though up to 18 CZCs are created. In the test case shown in Fig. 10, the VI has been arcing for about 4.3 ms until the last CZC. This could have been sufficient for the VI of type A to clear. Similar phenomena that the VI(s) fail to interrupt once re-ignitions/re-strikes occur are observed for the double interrupter tests of VI type C. In other words, this VI makes little attempt to interrupt the current after a re-ignition/re-strike.

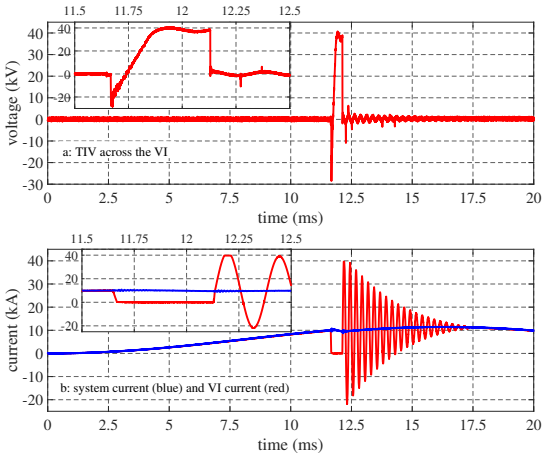

Fig. 10: Interruption failure after a re-strike in VI type C

Similar to the other VI types, the performance of a double interrupter dc CB composed VIs of type C is investigated. By far the main cause of re-ignitions/re-strikes in the double interrupter setups of types A and B VIs is unequal TIV distribution. In these cases 700 pF grading capacitors were put across each VI, see Fig. 3b. Evidently, this is not large enough to achieve equal voltage grading. Hence, in the double interrupter setup using VIs type C, the grading capacitors are increased to 2500 pF and this resulted in reasonably equal voltage sharing between the two serially connected VIs. First, 10 kA interruption tests are performed with arcing duration in the range between 1.18−1.34 ms. In all the cases the VIs cleared at the 1^{st} CZC. Then, high-current (16 kA) tests are performed. In this case, a few failures to interrupt, mainly caused by extremely short arcing durations, were recorded.

IV. Overall Statistics

Table III summarizes statistical information of the overall test results of each type of VIs. It can be seen that the VI of type A show by far the most number of re-ignitions and re-strikes with average of 5 re-ignitions per test. In fact only in 6.1% of the cases it cleared at the 1^{st} CZC. Nevertheless, it does not exhibit the highest failure rate among the three types of VIs. It must be noted that re-strikes in VI of type A do not lead to failed interruptions. Actually it clears the current in about 90% of the cases after a re-strike. Type B VI has the least re-strike rate but the highest failure rate. Most of the interruptions occurred at the 1^{st} CZC. Unlike for the VI of type A, for the of VI type C all the re-strikes led to failed current interruptions although the latter VI type has the highest rate of current interruption at the 1^{st} CZC.

TABLE III: Summary of Test Results of the three VCBs

VCB type	#tests	#CZCs	1^{st} CZC int.(%)	avg.# reign.	max.# reign.	restr. (%)	failure (%)
A	98	592	6.1	5.0	29	16.3	12.2
B	62	167	75.8	1.8	22	1.6	16.1
C	31	77	90.3	1.5	20	9.7	9.7

V. Conclusion

The paper presented dc fault current interruption performances of three different types of commercial ac VIs. Two test setups: the first using a single interrupter and the second using double interrupters are designed. Three interruption current magnitudes are defined and tests are performed at least 10 times while keeping the test parameters. Then, the test results are discussed in detail with a focus on the most critical parameters that have a strong impact on the current interruption performance. These parameters include the arcing duration until the CZCs, the rate-of-change of current near CZCs, and the initial and the peak values of the transient interruption voltage (TIV). Analysis of the test results shows that the three different types of VIs used in the investigation perform in a completely different manner when interrupting dc short-circuit currents. For example, VCB type A, rarely interrupts current on the 1^{st} CZC regardless of the length of arcing duration. This VI mainly interrupts the current on the even numbered CZCs which occur after minor loop current flow. On the other hand, the VCB type B mainly clears on the 1^{st} CZC. Re-ignitions occurred only on a few occasions and were subsequently cleared on later CZCs. Moreover, the third type of VCB, only clears on the 1^{st}

CZC. It never cleared when re-ignition occurred on the 1^{st} CZC or when a re-strike occurred afterward. These observations are supported by statistical analysis of the test results. In conclusion, this indicates a strong impact of the contact design, contact material and composition and pre-conditioning which are supposedly different for the investigated VIs. Hence, a VI can be optimized for dc current interruption. Moreover, re-ignitions and re-strikes are very common which entails that the test methods need to take into account adequate voltage stress across the insulation gap (vacuum, SF6, air) during the entire interruption process. Therefore, a special HVDC VI with very fast operating mechanism with the minimum scatter is essential to ensure sufficient contact gap (to avoid a re-ignition at the 1^{st} CZC) for a practical EHV/HVDC CB.

ACKNOWLEDGMENT

This project has received funding from the European Unions Horizon 2020 research and innovation programme under grant agreement No 691714.

REFERENCES

[1] CIGRE TB 683, *Technical Requirement and Specifications of State-of-the-art HVDC Switching Equipment*, CIGRE JWG A3/B4-34, March, 2017.

[2] S. Tokoyoda, T. Inagaki, R. Kamimae, K. Tahata, K. Kamei, T. Minagawa, D. Yoshida, H. Ito, “Development of EHV dc circuit breaker with current injection,” in *CIGRE-IEC 2019 Conference on EHV and UHV (AC & DC)*, Hakodate, Japan, 2019.

[3] N. A. Belda, C. Plet and R. P. P. Smeets, ”Full-Power Test of HVDC Circuit-Breakers with AC Short-Circuit Generators Operated at low Power Frequency”, in *IEEE Transactions on Power Delivery*, 2019, Early access articles.

[4] L. Ängquist, S. Nee, T. Modeer, A. Baudoin, S. Norrga and N. A. Belda, ”Design and test of VSC assisted resonant current (VARC) dc circuit breaker,” *15th IET International Conference on AC and DC Power Transmission (ACDC 2019)*, Coventry, UK, 2019, pp. 1-6.

[5] W. Grieshaber, J. -P. Dupraz, D. -L. Penache and L. Violleau, ”Development and test of a 120 kV direct current circuit breaker,” in *CIGRE Session* 45, B4-301, 2014.

[6] T. Eriksson, M. Backman and S. Halén, ”A low loss mechanical HVDC breaker for HVDC Grid applications,” in *CIGRE Session 45*, Paris, 2014.

[7] J. Häfner and B. Jacobson, ”Proactive Hybrid HVDC Breakers - A key innovation for reliable HVDC grids,” in *CIGRE Symposium*, Bologna, Italy , Sep 2011.

[8] W. Zhou, X. Wei, S. Zhang, G. Tang, Z. He and J. Zheng, ”Development and test of a 200kV full-bridge based hybrid HVDC breaker,” in *17th European Conference on Power Electronics and Applications (EPE’15 ECCE-Europe)*, Geneva, 2015.

[9] G. Tang, Z. He, H. Pang, X. Huang and X.-P. Zhang, ”Basic topology and key devices of the five-terminal DC grid,” *CSEE Journal of Power and Energy Systems*, vol. 1, no. 2, pp. 22-35, 2015.

[10] Z. Zhang, X. Li, M. Chen, et al., “Research and Development of 160kV Ultra-Fast Mechanical HVDC Circuit Breaker,” *Power System Technology*, Vol. 42, No. 7, pp. 23312338, 2018.

[11] H. Rao, ”Architecture of Nan’ao multi-terminal VSC-HVDC system and its multi-functional control,” *CSEE Journal of Power and Energy Systems*, vol. 1, no. 1, pp. 9-18, 2015.

[12] N. A. Belda, C. A. Plet and R. P. P. Smeets, ”Analysis of Faults in Multiterminal HVDC Grid for Definition of Test Requirements of HVDC Circuit Breakers”,*IEEE Transactions on Power Delivery*, vol. 33, no. 1, pp. 403 - 411, 2018.

[13] PROMOTioN Project Deliverable 5.3, “Fault Stress Analysis of HVDC Circuit Breakers,” PROMOTioN Project, 2016, available at https://www.promotion-offshore.net/results/deliverables/

[14] N. A. Belda, C. A. Plet, R. P. P. Smeets and R. M. Nijman, ”Stress Analysis of HVDC Circuit Breakers for Defining Test Requirements and its Implementation”, in *CIGRE Winnipeg 2017 Colloquium*, paper no. A3/B4-009, Winnipeg, Canada, 2017.

[15] N. A. Belda and R. P. P. Smeets, ”Test Circuits for HVDC Circuit Breakers,” *IEEE Transactions on Power Delivery*, vol. 32, no. 1, pp. 285 - 293, 2017.

[16] P. G. Slade, *The Vacuum Interrupter: Theory, Design, and Application*, 1^{st} edition, CRC Press,2007.

[17] A. Baudoin, B. Hátsági, M. Álvarez, L. Ängquist, S. Nee, S. Norrga, T. Modeer, “Experimental results from a Thomson-coil actuator for a vacuum interrupter in an HVDC breaker,” *The Journal of Engineering*, Available online: 26 April 2019